BRIDGING VISION AND LANGUAGE SPACES WITH ASSIGNMENT PREDICTION

Jungin Park[1], **Jiyoung Lee**[2*], **Kwanghoon Sohn**[1,3*]
[1]Yonsei University [2]NAVER AI Lab [3]Korea Institute of Science and Technology (KIST)
{newrun, khsohn}@yonsei.ac.kr lee.j@navercorp.com

ABSTRACT

This paper introduces VLAP, a novel approach that bridges pretrained vision models and large language models (LLMs) to make frozen LLMs a model of the non-linguistic visual world. VLAP transforms the embedding space of pretrained vision models into the LLMs' embedding space using a single linear layer, which is trained with the optimal transport-based assignment prediction objective. Specifically, we harness well-established word embeddings to bridge two modality embedding spaces. We simultaneously assign the visual and text representations to a set of word embeddings within pretrained LLMs through the optimal transport. We predict the assignment of one modality from the representation of another modality data, enforcing consistent assignments for paired multimodal data. This allows two modality representations to contain the same information, grounding the frozen LLMs' word embedding space in visual data. Moreover, a robust semantic taxonomy of LLMs can be preserved with visual data since the LLMs interpret and reason linguistic information from correlations between word embeddings. Experimental results show that VLAP achieves substantial improvements over the previous linear transformation-based methods across a range of vision-language tasks, including image captioning, visual question answering, and cross-modal retrieval. We also demonstrate the learned visual representations hold a semantic taxonomy of LLMs, making visual semantic arithmetic possible.

1 INTRODUCTION

Pretraining vision-language models (VLMs) has achieved significant progress in demonstrating remarkable transfer and zero-shot capabilities on vision-language downstream tasks (Tan & Bansal, 2019; Lu et al., 2019; Chen et al., 2020; Huang et al., 2020; Radford et al., 2021; Jia et al., 2021). Most cutting-edge VLMs have been developed with progressively scaled-up foundation models and datasets. This trend underscores the demand for substantial computational resources and an extensive collection of image-text pairs. Concurrently, pretrained unimodal foundation models, such as vision transformers (Bao et al., 2022; Caron et al., 2021) and large language models (LLMs) (Brown et al., 2020; Zhang et al., 2022; Raffel et al., 2020), have been developed, renewing the state-of-the-art in vision and language downstream tasks respectively. To build effective and computationally efficient VLMs, an interesting question has been drawn: Can pretrained unimodal models extend their capabilities beyond the modality of pretraining data?

Recently, intriguing attempts have been made to assemble pretrained vision models and LLMs to seem VLMs (Mokady et al., 2021; Tsimpoukelli et al., 2021; Alayrac et al., 2022; Patel & Pavlick, 2022; Eichenberg et al., 2022; Li et al., 2022; 2023; Guo et al., 2023). Most of these attempts suggested ways to train relatively small-scale connection modules while freezing pretrained parameters. By doing so, it is possible to efficiently make VLMs that leverage discriminative visual representations from pretrained image encoders, coupled with powerful language modeling and zero-shot capabilities of pretrained LLMs. While the burden of training costs in those methods has significantly decreased compared to pretraining VLMs, they still require high computations (both time and memory), which limits applicability (e.g. Flamingo (Alayrac et al., 2022) requires 15 days with

---

[*] Corresponding authors.

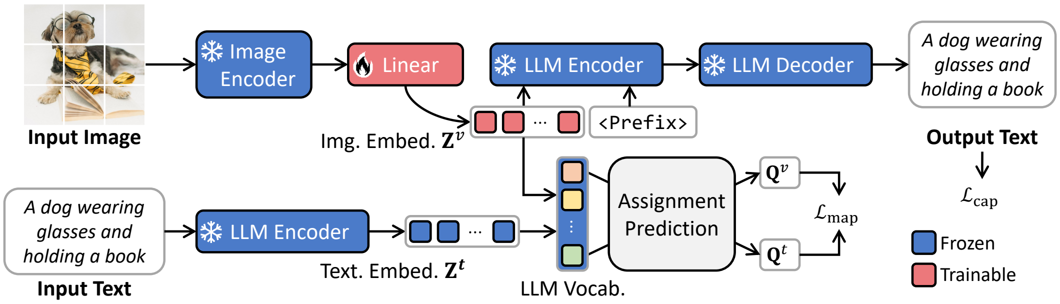
Input Image
Image Encoder
Linear
LLM Encoder
LLM Decoder
A dog wearing glasses and holding a book
Output Text
$\mathcal{L}_{\text{cap}}$
Img. Embed. $\mathbf{Z}^v$
<Prefix>
A dog wearing glasses and holding a book
Input Text
LLM Encoder
Text. Embed. $\mathbf{Z}^t$
LLM Vocab.
Assignment Prediction
$\mathbf{Q}^v$
$\mathbf{Q}^t$
$\mathcal{L}_{\text{map}}$
Frozen
Trainable

Figure 1: **Overview of VLAP**. We train a single linear layer following two learning objectives: Assignments prediction to bridge the modality gap between the visual and text representations; and image captioning to yield the generative capability of frozen LLMs.

1535 TPUs to train 10.2B parameters, BLIP-2 (Li et al., 2023) requires 9 days with 16 A100 GPUs to train 188M parameters).

Linear transformation-based approaches (Merullo et al., 2023; Koh et al., 2023) have facilitated efficient cross-modal alignment with a cost-efficient linear transformation between vision and language spaces. Merullo et al. (2023) has shown that visual representations can be linearly transformed into LLMs' input embedding as soft prompts, demonstrating that well-learned visual and text representations are functionally equivalent. Similarly, Koh et al. (2023) has proposed to generate free-form text interleaved with images by learning additional trainable tokens and linear layers. These linear transformation-based cross-modal alignments have been achieved by the image captioning and retrieval objectives, which directly compare the representations of image-text pairs and enforce instance discrimination as contrastive learning (Chopra et al., 2005). However, the inherent *modality gap* between different modality data leads to the inconsistency of the two models' embedding space (as their pretraining has been solely on unimodal data) and makes cross-modal alignment for frozen unimodal models difficult with the following challenges: (1) they are highly dependent on the amount of linguistic supervision used during pretraining of vision models, showing limited performance with vision-only image models (e.g. CLIP vs BEiT) (Merullo et al., 2023). (2) the contrastive objective (such as InfoNCE (van den Oord et al., 2018) in Koh et al. (2023)) is insufficient to bridge complex embedding spaces because it inherently encourages the existence of the modality gap (Liang et al., 2022).

In this paper, we propose a novel linear transformation-based method, which we call VLAP: bridging vision and language models with assignment prediction. VLAP learns a linear layer with a novel optimal transport-based assignment prediction that compares intermediate assignments for image and text data instead of directly comparing their representations. Specifically, visual and text representations are assigned to the most relevant word embeddings within pretrained LLMs using optimal transport. The assignment for one modality is predicted from the other modality representation, making two different modality representations contain the same linguistic information. We exploit the readily available word embedding space, following two main advantages: (1) it does not require additional learnable embedding space (e.g. prototypes in Asano et al. (2020b); Caron et al. (2020)) and (2) it allows visual representations to keep abundant linguistic contextual information and inherit a semantic taxonomy of LLMs. Our main contributions are four-fold:

- We propose a novel linear transformation-based method, called VLAP, to efficiently bridge pretrained image models and LLMs. VLAP employs an optimal transport-based assignment prediction objective to make visual and text representations compatible with each other.
- VLAP leverages the word embeddings of pretrained LLMs as a fixed central space for optimal transport. This allows us to easily bridge two pretrained frozen unimodal models by exploiting the fundamental components of LLMs.
- Mapping visual data to LLMs' word embeddings results in learned visual representations that hold a semantic taxonomy of LLMs, facilitating the operation in a textual way for visual data, e.g. visual semantic arithmetic operation.

- VLAP substantially outperforms existing linear transformation-based methods (Merullo et al., 2023; Koh et al., 2023) in a range of vision-language tasks, while also demonstrating high computational and memory efficiency.

2 RELATED WORK

Pretraining vision-language models (VLMs) Tan & Bansal (2019); Lu et al. (2019); Chen et al. (2020); Huang et al. (2020); Jia et al. (2021); Radford et al. (2021) has received tremendous interest thanks to their robust zero-shot capability for vision-language tasks such as image captioning, visual question answering, and cross-modal retrieval. Concurrently, in the past few years, large language models (LLMs) have achieved significant success in generating human-like language content with growth in model size and datasets at scale (Devlin et al., 2019; Radford et al., 2018; 2019; Brown et al., 2020; Raffel et al., 2020; Chung et al., 2022). To conjugate this ability of LLMs for vision-language research, recent works have attempted to adopt the visual embeddings as prompts of LLMs (Tsimpoukelli et al., 2021; Eichenberg et al., 2022; Mokady et al., 2021; Alayrac et al., 2022; Sung et al., 2022; Li et al., 2023). They accomplished this by tuning the visual encoder (Tsimpoukelli et al., 2021), introducing additional lightweight modules Mokady et al. (2021); Alayrac et al. (2022); Sung et al. (2022); Cohen et al. (2022); Li et al. (2023), or employing both approaches (Eichenberg et al., 2022).

Our work is highly related to LLaVA (Liu et al., 2023a), LiMBeR (Merullo et al., 2023), and FROMAGe (Koh et al., 2023). Different from the modular-based methods, which require relatively a high computational cost, they presented a linear transformation-based approach to project visual embeddings into the text embedding space using only linear transformations. They demonstrated that vision models and LLMs share non-trivial similar information even though two unimodal models are trained independently. However, their learning objectives, which directly compare the visual and text representations, are restrictive solutions to bridge the modality gap (Liang et al., 2022). Unlike the previous methods, we compare the assignments between image and text data by formulating an optimal transport-based assignment prediction with word embeddings of pretrained LLMs. We demonstrate that the modality gap between pretrained vision models and LLMs can be effectively bridged while preserving high computational efficiency with the proposed assignment prediction.

3 METHOD

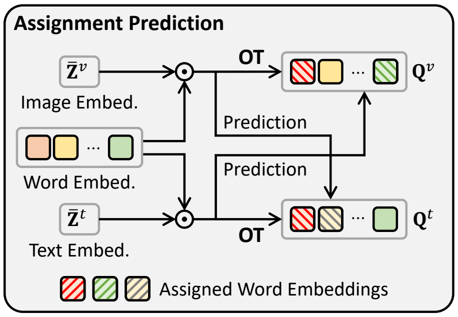

Figure 2: **Assignment prediction.** The modality gap can be relaxed by predicting the word assignments of one modality from the other modality representations.

Our primary goal is to make pretrained LLMs comprehend visual inputs with minimum training for vision-language tasks. More precisely, we aim to bridge pretrained vision models and LLMs using by learning only a linear layer (i.e., keeping the original parameters frozen) while preserving the representative power of pretrained vision models and the generalization ability of pretrained LLMs. To this end, we proposed a novel linear transformation-based method VLAP: bridging vision and language models with assignment prediction. The key component to bridge pretrained vision and language models is mapping information between image and text representations to make frozen LLMs interpret visual inputs as linguistic components. The previous linear transformation-based methods (Merullo et al., 2023; Koh et al., 2023) linearly transform the visual representation from pretrained image encoder into LLMs' embedding space and directly compare representations of paired multimodal data. In contrast, we resolve the linear cross-modal alignment using assignment prediction (Asano et al., 2020b; Caron et al., 2020) that compares intermediate assignments to enforce consistent assignments to multimodal data. VLAP learns a linear layer by optimizing two objectives simultaneously: (1) optimal transport-based assignment prediction to enforce the visual and text representations contain the same information and (2) image-to-text generation to incorporate the visual representation into the generative ability of LLMs. This section introduces each component in detail, and the overview of VLAP is shown in Figure 1.

3.1 ASSIGNMENT PREDICTION

We first assign visual and text representations into word embeddings using optimal transport as if each data is clustered into the word embedding space of pretrained LLMs. The proposed assignment prediction is performed to predict each other's assignments. We notice that recent works for the assignment prediction problem formulate a set of learnable embeddings (i.e., prototypes) to cluster the given data into them (Caron et al., 2020; Xu et al., 2020; Liu et al., 2023b; Duan et al., 2022), requiring additional memory and gradient computation. Contrary to this, VLAP utilizes readily available word embeddings of LLMs. By employing the pretrained word embedding space of LLMs as a fixed central space into which visual representations are mapped, the training process is more stable and memory-efficient.

Visual and text representations from pretrained models. Given a set of B images, we extract the last hidden state from pretrained image encoder as the visual representations $\mathbf{X} = \{\mathbf{X}_1, ..., \mathbf{X}_B\}$, where the representation for each image contains d_v-dimensional N_p feature vectors, i.e., $\mathbf{X}_n = \{\mathbf{x}_n^1, ..., \mathbf{x}_n^{N_p}\} \in \mathbb{R}^{N_p \times d_v}$. Similarly, we feed a set of B captions corresponding to the images into pretrained LLM to obtain the text representations $\mathbf{Z}^t = \{\mathbf{Z}_1^t, ..., \mathbf{Z}_B^t\}$, where $\mathbf{Z}_n^t = \{\mathbf{z}_n^{t,1}, ..., \mathbf{z}_n^{t,T_n}\} \in \mathbb{R}^{T_n \times d}$, T_n is the number of words in the n-th caption, and d is the embedding dimension of LLM.

Word assignment. We project the visual representations $\mathbf{X}$ into the same dimension as the embedding space of LLMs using a linear layer $g(\cdot)$:

$$\mathbf{Z}^v = \{\mathbf{Z}_n^v \in \mathbb{R}^{N_p \times d} \mid \mathbf{Z}_n^v = g(\mathbf{X}_n), n = 1, ..., B\}. \tag{1}$$

We assign the image and text to a set of words by mapping the averaged visual and text representations to the frozen word embeddings $\mathbf{W} = \{\mathbf{w}_1, ..., \mathbf{w}_K\}$ of LLM, where K is a vocabulary size. Similar to the prior works (Asano et al., 2020b; Caron et al., 2020), we simultaneously optimize the assignment $\mathbf{Q}^v = \{\mathbf{q}_1^v, ..., \mathbf{q}_B^v\}$ and $\mathbf{Q}^t = \{\mathbf{q}_1^t, ..., \mathbf{q}_B^t\}$ to maximize the similarity between the representations for each modality and the word embeddings:

$$\begin{gathered}\max_{\mathbf{Q}^v \in \mathcal{Q}} \text{Tr}(\mathbf{Q}^{v\top}\mathbf{W}^\top\bar{\mathbf{Z}}^v) + \epsilon H(\mathbf{Q}^v), \quad \max_{\mathbf{Q}^t \in \mathcal{Q}} \text{Tr}(\mathbf{Q}^{t\top}\mathbf{W}^\top\bar{\mathbf{Z}}^t) + \epsilon H(\mathbf{Q}^t), \\ \text{where} \quad \bar{\mathbf{Z}}^v = \{\bar{\mathbf{z}}_1^v, ..., \bar{\mathbf{z}}_B^v\}, \quad \bar{\mathbf{z}}_n^v = \frac{1}{N_p}\sum_i \mathbf{z}_n^{v,i}, \quad \bar{\mathbf{Z}}^t = \{\bar{\mathbf{z}}_1^t, ..., \bar{\mathbf{z}}_B^t\}, \quad \bar{\mathbf{z}}_n^t = \frac{1}{T_b}\sum_i \mathbf{z}_n^{t,i}.\end{gathered} \tag{2}$$

We denote the trace matrix as Tr($\cdot$), entropy function as $H(\mathbf{Q}) = -\sum_{ij}\mathbf{Q}_{ij}\log\mathbf{Q}_{ij}$, and a smoothness parameter of the mapping as ϵ. The previous methods assume that all samples are equally assigned to each cluster by constraining the matrix $\mathbf{Q}$ to belong to the transportation polytope in the whole dataset (Asano et al., 2020b) or the minibatch (Caron et al., 2020). However, the equipartition assumption can lead to impractical solutions in our work since the numbers of words are not equally distributed in practice. Therefore, we restrict the transportation polytope with the following constraints:

$$\mathcal{Q} = \{\mathbf{Q} \in \mathbb{R}_+^{K \times B} \mid \mathbf{Q}\mathbf{1}_B = \boldsymbol{\mu}_W, \mathbf{Q}^\top\mathbf{1}_K = \frac{1}{B}\mathbf{1}_B\}, \tag{3}$$

where $\mathbf{1}_B$ denotes the vector of ones in dimension B and $\boldsymbol{\mu}_W$ is the marginal distribution of words, i.e., $\boldsymbol{\mu}_W(k) = \frac{N_k}{\sum_{k'} N_{k'}}$, where N_k denotes the total number of the k-th word in the dataset. Formally, $\boldsymbol{\mu}_W$ can be represented as a vector with the length of LLM's vocabulary size (e.g., 50,272 for OPT (Zhang et al., 2022), 32,128 for T5 (Raffel et al., 2020)). By satisfying the constraints, the word embeddings are selected according to their frequency in the dataset. The optimized assignments $\mathbf{Q}^{v*}$ and $\mathbf{Q}^{t*}$ can be obtained over the set $\mathcal{Q}$ as the form of a normalized exponential matrix (Cuturi, 2013):

$$\mathbf{Q}^{v*} = \text{Diag}(\boldsymbol{\mu}_W)\exp\left(\frac{\mathbf{W}^\top\bar{\mathbf{Z}}^v}{\epsilon}\right)\text{Diag}(\mathbf{c}), \quad \mathbf{Q}^{t*} = \text{Diag}(\boldsymbol{\mu}_W)\exp\left(\frac{\mathbf{W}^\top\bar{\mathbf{Z}}^t}{\epsilon}\right)\text{Diag}(\mathbf{c}), \tag{4}$$

where $\mathbf{c}$ is a re-normalized vector in $\mathbb{R}^B$ obtained using the iterative Sinkhorn-Knopp algorithm (Cuturi, 2013).

Method	Vis. Encoder	Lang. Model	NoCaps (CIDEr-D)				NoCaps (All)		MSCOCO		
			In	Out	Near	All	CLIP-S	Ref-S	CIDEr-D	CLIP-S	Ref-S
MAGMA	CLIP RN50x16	GPT-J	30.4	43.4	36.7	38.7	74.3	78.7	47.5	75.3	79.6
LiMBeR	BEiT	GPT-J	20.3	16.3	26.9	28.5	62.0	69.1	22.3	63.6	70.0
LiMBeR	CLIP RN50x16	GPT-J	34.3	48.4	41.6	43.9	74.7	79.4	54.9	76.2	80.4
VLAP	BEiT	$\text{OPT}_{1.3\text{B}}$	31.1	45.4	40.6	42.2	72.1	77.3	50.7	73.7	76.4
VLAP	BEiT	T5_{Base}	31.6	46.3	41.9	43.4	72.6	78.9	51.6	74.2	78.5
VLAP	CLIP ViT-B/32	$\text{OPT}_{1.3\text{B}}$	48.2	**62.7**	59.3	61.3	84.8	88.5	**69.9**	86.7	91.8
VLAP	CLIP ViT-B/32	T5_{Base}	**48.3**	**62.7**	**59.6**	**61.6**	**85.1**	**88.7**	69.4	**87.6**	**92.0**

Table 1: Performance comparisons between MAGMA (Eichenberg et al., 2022), LiMBeR (Merullo et al., 2023), and VLAP for zero-shot image captioning on the NoCaps and MSCOCO datasets. We report the architectures of visual and language models, CIDEr-D (Vedantam et al., 2015), CLIP-Score, and RefCLIP Score (Hessel et al., 2021).

Relaxing the modality gap with assignment prediction. The objective of our method is to predict the assignment of one modality from the other modality representation, i.e., predicting $\mathbf{Q}^v$ from $\bar{\mathbf{Z}}^t$ and $\mathbf{Q}^t$ from $\bar{\mathbf{Z}}^v$. The assignment prediction can be formulated with the cross-entropy loss between the assignment and the probability that the corresponding modality data belongs to each word:

$$\begin{aligned}\mathcal{L}_{\text{map}} &= -\frac{1}{B}\sum_{n=1}^{B}\sum_{k=1}^{K}[\mathbf{Q}^t_{nk}\log \mathbf{P}^v_{nk} + \mathbf{Q}^v_{nk}\log \mathbf{P}^t_{nk}], \\ \text{where}\quad \mathbf{P}^m_{nk} &= \frac{\exp(\bar{\mathbf{z}}_n^\top \mathbf{w}_k/\tau)}{\sum_{k'}\exp(\bar{\mathbf{z}}_n^\top \mathbf{w}_{k'}/\tau)}, \quad m \in \{v, t\},\end{aligned} \tag{5}$$

where τ is a temperature parameter (Wu et al., 2018). This loss function makes two different modality representations contain the same information.

3.2 IMAGE CAPTIONING WITH FROZEN LLMS

To connect the (projected) visual representations to a frozen LLM to yield the general capability of LLM (i.e., generative ability), we train the linear projection layer $g(\cdot)$ with the image captioning objective. Specifically, the visual representations $\mathbf{Z}_v$ are prepended to the input text prompt (e.g. "`A photo of`"), being active as soft prompts of LLM. Following the previous works (Merullo et al., 2023; Koh et al., 2023), we employ the prefix language modeling loss as the objective:

$$\mathcal{L}_{\text{cap}} = -\frac{1}{B}\sum_{n=1}^{B}\frac{1}{N_t}\sum_{t=1}^{N_t}\log f_t(s_t \mid \mathbf{Z}^v_n, [\texttt{prefix}], s_1, ..., s_{t-1}), \tag{6}$$

where N_t is the number of words in the caption, `[prefix]` is the input text prompt, and s_t is a text token of the t-th word.

The final objective function is a weighted sum of the assignment prediction loss and captioning loss:

$$\mathcal{L} = \lambda_{\text{map}}\mathcal{L}_{\text{map}} + \lambda_{\text{cap}}\mathcal{L}_{\text{cap}}, \tag{7}$$

where λ_{map} and λ_{cap} control the importance of each objective. By minimizing the final objective, we simultaneously make the visual and text representations contain the same information while keeping the capability of LLM, allowing the frozen image encoder and LLM can be effectively connected with only the linear transformation.

4 EXPERIMENTS

4.1 EXPERIMENTAL SETTINGS

We define the transport polytope in the assignment prediction with the word distribution of a given dataset. This assumption poses one possible problem: VLAP often fails when the word distribution of training data cannot cover real-world scenarios. However, to prevent the assignments from being

Method	Vis.Encoder	Lang. Model	n-shots			
			0	1	2	4
Frozen	NFRN50	GPT-2	29.5	35.7	-	38.2
MAGMA	CLIP RN50x16	GPT-J	32.7	40.2	42.5	43.8
LiMBeR	BEiT	GPT-J	24.9	34.4	34.7	31.7
LiMBeR	CLIP RN50x16	GPT-J	33.3	39.9	40.8	40.3
VLAP	BEiT	$\text{OPT}_{1.3\text{B}}$	34.5	44.2	45.1	45.7
VLAP	BEiT	T5_{Base}	34.7	43.3	45.4	45.5
VLAP	CLIP ViT-B/32	$\text{OPT}_{1.3\text{B}}$	40.4	**52.6**	**53.8**	**54.7**
VLAP	CLIP ViT-B/32	T5_{Base}	**41.1**	51.3	51.9	52.6

Table 2: Performance comparisons between Frozen (Tsimpoukelli et al., 2021), MAGMA (Eichenberg et al., 2022), LiMBeR (Merullo et al., 2023), and VLAP for zero-shot visual question answering on the VQA2 datasets. We report the architectures of visual and language models and accuracy (%).

Method	Train. Params.	Finetune Data	IT2T					T2I		
			NDCG	MRR	R@1	R@5	R@10	R@1	R@5	R@10
ViLBERT	114M	3.1M	11.6	6.9	2.6	7.2	11.3	-	-	-
CLIP ViT-L/14	300M	400M	10.9	8.5	3.1	8.7	15.9	17.7	38.9	50.2
ESPER	4M	0.5M	22.3	**25.7**	14.6	-	-	Incapable		
FROMAGe	5.5M	3.1M	16.5	22.0	17.6	20.1	25.1	20.8	44.9	56.0
VLAP w/CLIP-T5_{Base}	0.6M	3.1M	20.5	24.9	**21.1**	**23.7**	**29.6**	**26.9**	**55.3**	**69.1**

Table 3: Performance comparisons between ViLBERT (Lu et al., 2019), CLIP (Radford et al., 2021), ESPER (Yu et al., 2022), FROMAGe (Koh et al., 2023), and VLAP for zero-shot image-and-text-to-text (IT2T) and text-to-image (T2I) retrieval on the Visual Dialog datasets. Following Koh et al. (2023), we report Normalized Discounted Cumulative Gain (NDCG), Mean Reciprocal Recall (MRR), R@1, R@5, and R@10 for IT2T retrieval and R@1, R@5, and R@10 for T2I retrieval.

collapsed to the word distribution, we preserve the soft assignments as in Caron et al. (2020). In addition, we carefully argue that a large dataset (e.g. CC3M (Sharma et al., 2018)) is sufficient to cover the real-world scenario. To validate this, we mainly investigate vision-language tasks with the zero-shot setting, i.e., training and test data come from different datasets.

Datasets. We evaluate VLAP on three vision-language tasks, including zero-shot image captioning, visual question answering (VQA), and cross-modal retrieval. We first train the model on the CC3M (Sharma et al., 2018) and evaluate the performance on the following datasets for each task. For zero-shot image captioning, we evaluate the performance on MSCOCO (Lin et al., 2014) and NoCaps (Agrawal et al., 2019), following (Merullo et al., 2023). For visual question answering, we evaluate the model on the VQA2 (Goyal et al., 2017) dataset from zero-shot to 4-shot settings. In cross-modal retrieval, we use the Visual Dialog (Das et al., 2017) dataset for the comparability to previous work (Koh et al., 2023).

Model architecture. For the frozen image encoders, we employ two different pretrained vision transformer models according to their pretraining data configuration: BEiT (Bao et al., 2022) pretrained on image-only data and CLIP ViT/B-32 (Radford et al., 2021) jointly learned with the text encoder on image-text data. For the frozen language models, we explore two types of LLMs according to their architectural configuration: $\text{OPT}_{1.3\text{B}}$ (Zhang et al., 2022) as decoder-based LLMs and T5_{Base} (Raffel et al., 2020) as encoder-decoder-based LLMs.

4.2 ZERO-SHOT IMAGE CAPTIONING

We provide performance comparisons between Frozen (Tsimpoukelli et al., 2021), MAGMA (Eichenberg et al., 2022), LiMBeR (Merullo et al., 2023), and VLAP for zero-shot image captioning in Table 1. We mainly report CIDEr-D (Vedantam et al., 2015), CLIPScore, and Ref-CLIPScore (Hessel et al., 2021), following (Merullo et al., 2023). The results show that VLAP consistently outperforms the previous linear transformation-based approach (Merullo et al.,

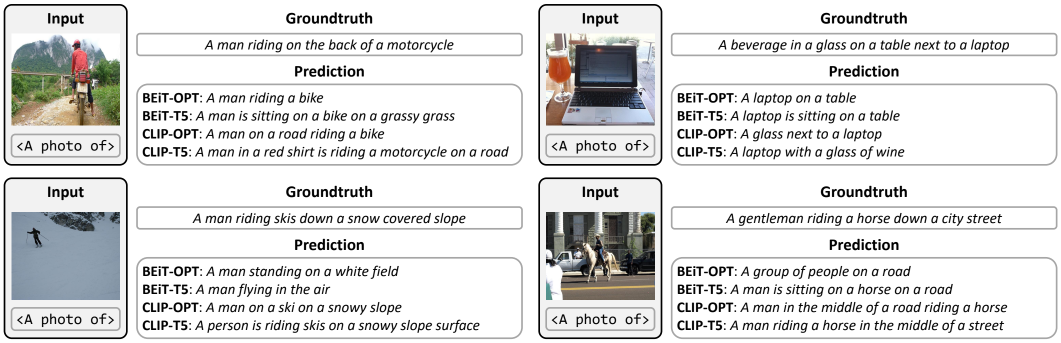

A man riding on the back of a motorcycle

BEiT-OPT: *A man riding a bike*
BEiT-T5: *A man is sitting on a bike on a grassy grass*
CLIP-OPT: *A man on a road riding a bike*
CLIP-T5: *A man in a red shirt is riding a motorcycle on a road*

A beverage in a glass on a table next to a laptop

BEiT-OPT: *A laptop on a table*
BEiT-T5: *A laptop is sitting on a table*
CLIP-OPT: *A glass next to a laptop*
CLIP-T5: *A laptop with a glass of wine*

A man riding skis down a snow covered slope

BEiT-OPT: *A man standing on a white field*
BEiT-T5: *A man flying in the air*
CLIP-OPT: *A man on a ski on a snowy slope*
CLIP-T5: *A person is riding skis on a snowy slope surface*

A gentleman riding a horse down a city street

BEiT-OPT: *A group of people on a road*
BEiT-T5: *A man is sitting on a horse on a road*
CLIP-OPT: *A man in the middle of a road riding a horse*
CLIP-T5: *A man riding a horse in the middle of a street*

(a) Zero-shot image captioning

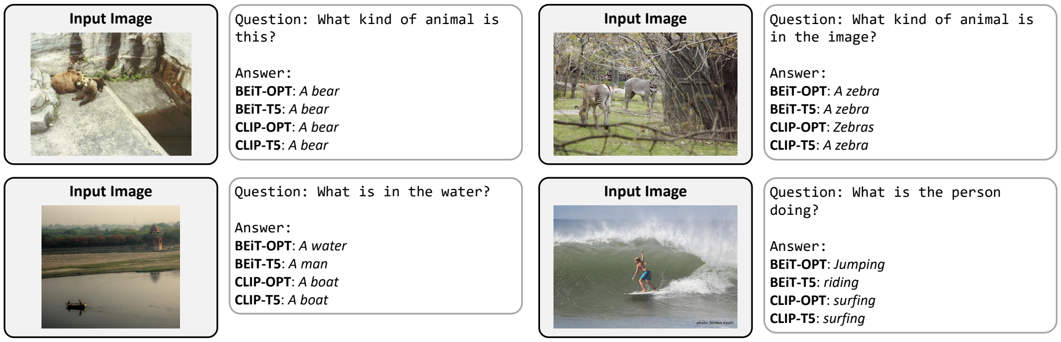

Question: What kind of animal is this?
Answer:
BEiT-OPT: *A bear*
BEiT-T5: *A bear*
CLIP-OPT: *A bear*
CLIP-T5: *A bear*

Question: What kind of animal is in the image?
Answer:
BEiT-OPT: *A zebra*
BEiT-T5: *A zebra*
CLIP-OPT: *Zebras*
CLIP-T5: *A zebra*

Question: What is in the water?
Answer:
BEiT-OPT: *A water*
BEiT-T5: *A man*
CLIP-OPT: *A boat*
CLIP-T5: *A boat*

Question: What is the person doing?
Answer:
BEiT-OPT: *Jumping*
BEiT-T5: *riding*
CLIP-OPT: *surfing*
CLIP-T5: *surfing*

(b) Visual question answering

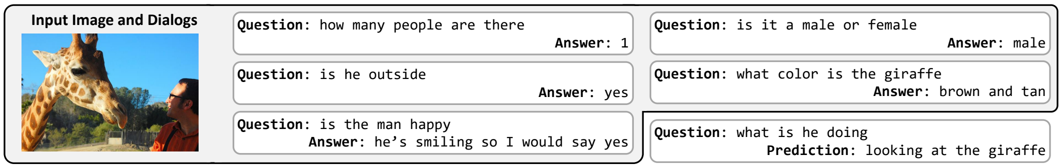

Question: how many people are there **Answer**: 1
Question: is he outside **Answer**: yes
Question: is the man happy **Answer**: he's smiling so I would say yes
Question: is it a male or female **Answer**: male
Question: what color is the giraffe **Answer**: brown and tan
Question: what is he doing **Prediction**: looking at the giraffe

(c) Visual dialog (image-and-text to text (IT2T) retrieval)

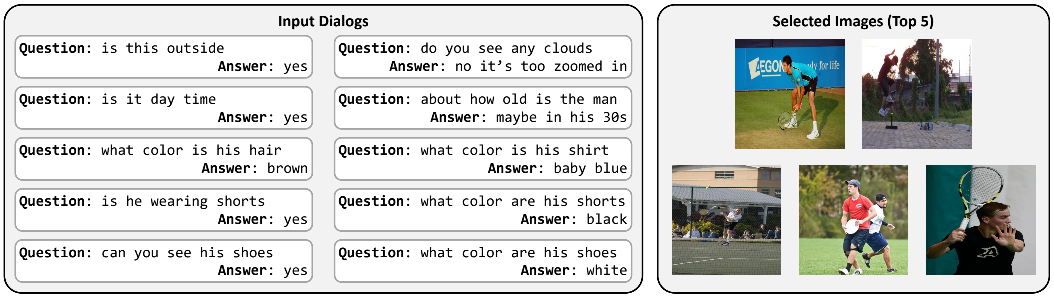

Question: is this outside **Answer**: yes
Question: is it day time **Answer**: yes
Question: what color is his hair **Answer**: brown
Question: is he wearing shorts **Answer**: yes
Question: can you see his shoes **Answer**: yes
Question: do you see any clouds **Answer**: no it's too zoomed in
Question: about how old is the man **Answer**: maybe in his 30s
Question: what color is his shirt **Answer**: baby blue
Question: what color are his shorts **Answer**: black
Question: what color are his shoes **Answer**: white

(d) Text-to-image retrieval

Figure 3: Selected examples from VLAP for vision-language tasks, including (a) zero-shot image captioning, (b) visual question answering (VQA), (c) visual dialog, and (d) text-to-image (T2I) retrieval.

2023) with large margins. Especially, VLAP with the BEiT with T5_{Base} achieves 14.9% and 29.3% CIDEr-D improvements on each dataset. Remarkably, it achieves comparable performance to LiMBeR with the CLIP image encoder, despite BEiT lacking linguistic supervision in its pretraining. VLAP also attains significantly higher CLIPScores, which represent how the image and generated caption are semantically similar, improving the CLIP-S by 10.4%, 11.4%, and the RefCLIP-S by 9.3%, 11.6% on NoCaps and MSCOCO, respectively. In addition, we use a much smaller number of parameters in LLMs (T5_{Base} has 220M parameters, while GPT-J has 6B parameters), demonstrating the effectiveness of the proposed method in grounding LLMs to visual data. The performance evaluated with additional captioning metrics, including BLEU (Papineni et al., 2002), METEOR (Banerjee & Lavie, 2005), ROUGE (Lin, 2004), and SPICE (Anderson et al., 2016), are shown in Appendix C.

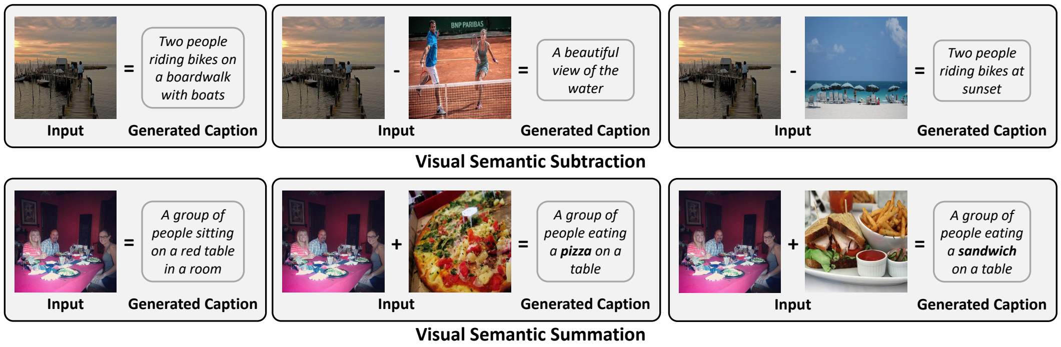
Input
=
Two people riding bikes on a boardwalk with boats
Generated Caption
Input
-
=
A beautiful view of the water
Generated Caption
Input
-
=
Two people riding bikes at sunset
Generated Caption
Visual Semantic Subtraction
Input
=
A group of people sitting on a red table in a room
Generated Caption
Input
+
=
A group of people eating a **pizza** on a table
Generated Caption
Input
+
=
A group of people eating a **sandwich** on a table
Generated Caption
Visual Semantic Summation

Figure 4: Selected examples for visual semantic arithmetic.

We also provide the qualitative examples in Figure 3a. The results show impressive performance of VLAP across all vision-language models. Even when applied to BEiT, it consistently generates accurate captions, even if occasionally produces relatively simplified captions and provides some wrong cases (e.g. 'snow' as 'white field' or 'air' in the example).

4.3 VISUAL QUESTION ANSWERING

We evaluate the performance with zero-shot and few-shot settings[1] on visual question answering (VQA). In n-shot settings, we randomly prepend n complete examples before each question as described in Tsimpoukelli et al. (2021); Eichenberg et al. (2022). We use the text prompt "`Question: {} Answer:`" for the OPT model and "`Question: {} Short Answer:`" for the T5 model, following Li et al. (2023). We provide the comparison between VLAP and three baselines (Tsimpoukelli et al., 2021; Eichenberg et al., 2022; Merullo et al., 2023), as shown in Table 2. VLAP outperforms the previous methods with large margins, showing the effectiveness of the proposed method. Surprisingly, VLAP with the BEiT and T5$_{\text{Base}}$, which is the most challenging condition (in terms of pretraining data and the number of parameters), achieves higher performance than the previous methods for all evaluation settings.

In Figure 3b, we provide the qualitative examples for zero-shot and 4-shot VQA. For zero-shot VQA, the results show that while VLAP generally infers the correct answers with all image encoders and language models, some failure cases are shown with the BEiT models.

4.4 CROSS-MODAL RETRIEVAL

For cross-modal retrieval, we compare the performance of ViLBERT (Lu et al., 2019), CLIP (Radford et al., 2021), ESPER (Yu et al., 2022), FROGMAGe (Koh et al., 2023), and VLAP evaluated on Visual Dialog (Das et al., 2017) for two types of retrieval tasks: (1) visual dialog referred to as image-and-text-to-text (IT2T) retrieval to reason the correct answer from given an image, a question, and a dialog about an image. We report the Normalized Discounted Cumulative Gain (NDCG), Mean Reciprocal Recall (MRR), and Recall@k, following Yu et al. (2022); Koh et al. (2023). (2) text-to-image (T2I) retrieval to find the image from a given dialog. We report the Recall@k performance for T2I retrieval. Since a dialog in the dataset consists of question-answer pairs for images, we use the text prompt used in the VQA task. We provide the comparisons for cross-modal retrieval in Table 3.

Image-and-text to text (IT2T) retrieval. For IT2T retrieval, we compute the loss (i.e. cross-entropy loss) between the prediction and given answer candidates, and select the answer with the lowest loss. VLAP outperforms the previous methods (Lu et al., 2019; Radford et al., 2021; Yu et al., 2022; Koh et al., 2023), achieving 3.5%, 3.6%, and 4.5% improvements on R@1, 5, and 10, respectively. While VLAP shows slightly lower NDCG and MRR performance than ESPER (Yu et al.,

---

[1] We follow the procedure of the official VQA 2.0 repo: `https://github.com/GT-Vision-Lab/VQA`.

2022), they train the model on the superset of Visual Dialog (i.e. MSCOCO), already containing in-context information of the dataset. The comparison between VLAP and FROMAGe demonstrates the effectiveness of our assignment prediction objective as the main difference between the two methods is the learning objective. VLAP consistently outperforms FROMAGe (Koh et al., 2023) even with fewer trainable parameters, improving 4.0% and 2.9% on NDGC and MRR, respectively.

Text-to-image (T2I) retrieval. As VLAP minimizes the modality gap between image and text data, the visual and text representations can be directly used to retrieve each other. For T2I retrieval, we first extract the text and visual representation for a given dialog and all images in the dataset. We directly measure the similarity between the text and visual representations and select the image with the highest similarity. VLAP substantially outperforms the prior works (Radford et al., 2021; Koh et al., 2023) over all evaluation metrics, achieving 9.2% and 6.1% improvements on R@1 over CLIP (Radford et al., 2021) and FROMAGe.

The experiments on cross-modal retrieval demonstrate the flexibility of VLAP for vision-language tasks. We emphasize that VLAP provides competitive results even on the retrieval task, showing that VLAP can be applied as a general model without being limited to tasks.

4.5 VISUAL SEMANTIC ARITHMETIC

The pretrained LLMs capture task-agnostic linguistic structures and lexical semantics (Jawahar et al., 2019; Liu et al., 2019; Tenney et al., 2019; Hewitt & Manning, 2019; Vulić et al., 2019). Recent work (Tewel et al., 2022) has shown this capability persists in VLMs (e.g. CLIP model) so that the visual embeddings can be expressed in a textual way, which is called visual semantic arithmetic. For example, the semantic direction between two images can be expressed by subtracting one visual representation from another visual representation. Similarly, the summation of two visual representations allows for guidance for text generation. Even though we leverage independently pretrained image encoders and LLMs, the visual representations learned to be projected into the word embedding space, holding a semantic taxonomy of LLMs. To demonstrate the arithmetical ability of VLAP, we provide an analysis of visual semantic arithmetic (i.e., subtraction and summation operations), as shown in Figure 4.

In subtraction, the conceptual direction between two images can be obtained. For example, “A beautiful view of the water” and “Two people riding bikes at sunset” are obtained from the same image of “Two people riding bikes on a boardwalk with boats” by subtracting images containing “two people” and “view of the ocean,” respectively. Meanwhile, the visual concepts can be guided by other visual semantics with summation operations. For example, a scene of people sitting around a table can be guided by the image of “pizza” and “sandwich”, generating a caption of “A group of people eating a pizza (or sandwich) on a table”. These results demonstrate that the visual representations from VLAP contain the semantic taxonomy of LLMs, allowing the VLAP’s visual representations to be expressed in a textual way.

5 CONCLUSION AND FUTURE WORK

We propose VLAP, a novel linear transformation-based method that bridges pretrained vision encoders and LLMs using a single linear layer for vision-language tasks. VLAP efficiently and effectively learns the linear mapping between image and text data by formulating optimal transport-based assignment prediction using LLMs’ word embeddings. We show that VLAP holds a semantic taxonomy of LLMs, presenting the emerging flexibility and applicability of the proposed method. VLAP achieves substantial performance improvement over the previous linear transformation-based methods on various vision-language tasks, demonstrating the effectiveness of VLAP.

While linear transformation-based methods have extremely high computation and memory efficiency, there is still a substantial performance gap against modular-based methods, such as Flamingo and BLIP-2. We attribute such gap to a lot of trainable parameters in their methods (10.2B in Flamingo, 188M in BLIP-2) and larger training data (1.8B image-text pair in Flamingo, 129M image-text pair in BLIP-2). Since the optimal transport-based assignment prediction can be easily moved to the modular-based methods, scaling VLAP with the modular-based models and training on larger multimodal datasets are promising directions for future work.

6 REPRODUCIBILITY STATEMENT

VLAP employs the pretrained BEiT and CLIP image encoder as vision models and the pretrained $\text{OPT}_{1.3\text{B}}$ and T5_{Base} as LLMs, which can be accessed by anyone. We provide PyTorch implementation for VLAP at `https://github.com/park-jungin/vlap`. The implementations will enable researchers to reproduce the results demonstrated in the paper as well as conduct additional analysis for VLAP with other vision models and LLMs.

ACKNOWLEDGEMENT

This research was supported by the National Research Foundation of Korea (NRF) grant funded by the Korea government (MSIP) (NRF2021R1A2C2006703).

REFERENCES

Harsh Agrawal, Karan Desai, Yufei Wang, Xinlei Chen, Rishabh Jain, Mark Johnson, Dhruv Batra, Devi Parikh, Stefan Lee, and Peter Anderson. Nocaps: Novel object captioning at scale. In *ICCV*, 2019.

Jean-Baptiste Alayrac, Jeff Donahue, Pauline Luc, Antoine Miech, Iain Barr, Yana Hasson, Karel Lenc, Arthur Mensch, Katie Millican, Malcolm Reynolds, Roman Ring, Eliza Rutherford, Serkan Cabi, Tengda Han, Zhitao Gong, Sina Samangooei, Marianne Monteiro, Jacob Menick, Sebastian Borgeaud, Andrew Brock, Aida Nematzadeh, Sahand Sharifzadeh, Mikolaj Binkowski, Ricardo Barreira, Oriol Vinyals, Andrew Zisserman, and Karen Simonyan. Flamingo: a visual language model for few-shot learning. In *NeurIPS*, 2022.

Peter Anderson, Basura Fernando, Mark Johnson, and Stephen Gould. Spice: Semantic propositional image caption evaluation. In *ECCV*, 2016.

Yuki M. Asano, Mandela Patrick, Christian Rupprecht, and Andrea Vedaldi. Labelling unlabelled videos from scratch with multi-modal self-supervision. In *NeurIPS*, 2020a.

Yuki M. Asano, Christian Rupprecht, and Andrea Vedaldi. Self-labelling via simultaneous clustering and representation learning. In *ICLR*, 2020b.

Satanjeev Banerjee and Alon Lavie. Meteor: An automatic metric for mt evaluation with improved correlation with human judgments. In *ACL Workshop*, 2005.

Hangbo Bao, Li Dong, Songhao Piao, and Furu We. Beit: Bert pertaining of image transformers. In *ICLR*, 2022.

Tom B. Brown, Benjamin Mann, Nick Ryder, Melanie Subbiah, Jared Kaplan, Prafulla Dhariwal, Arvind Neelakantan, Pranav Shyam, Girish Sastry, Amanda Askell, Sandhini Agarwal, Ariel Herbert-Voss, Gretchen Krueger, Tom Henighan, Rewon Child, Aditya Ramesh, Daniel M. Ziegler, Jeffrey Wu, Clemens Winter, Christopher Hesse, Mark Chen, Eric Sigler, Mateusz Litwin, Scott Gray, Benjamin Chess, Jack Clark, Christopher Berner, Sam McCandlish Alec Radford, Ilya Sutskever, and Dario Amodei. Language models are few-shot learners. In *NeurIPS*, 2020.

Mathilde Caron, Ishan Misra, Julien Mairal, Priya Goyal, Piotr Bojanowski, and Armand Joulin. Unsupervised learning of visual features by contrasting cluster assignments. In *NeurIPS*, 2020.

Mathilde Caron, Hugo Touvron, Ishan Misra, Hervé Jégou, Julien Mairal, Piotr Bojanowski, and Armand Joulin. Emerging properties in self-supervised vision transformers. In *CVPR*, 2021.

Soravit Changpinyo, Piyush Sharma, Nan Ding, and Radu Soricut. Conceptual 12m: Pushing web-scale image-text pre-training to recognize long-tail visual concepts. In *CVPR*, 2021.

Yen-Chun Chen, Linjie Li, Licheng Yu, Ahmed El Kholy, Faisal Ahmed, Zhe Gan, Yu Cheng, and Jingjing Liu. Uniter: Universal image-text representation learning. In *ECCV*, 2020.

Sumit Chopra, Raia Hadsell, and Yann LeCun. Learning a similarity metric discriminatively, with application to face verification. In *CVPR*, 2005.

Hyung Won Chung, Le Hou, Shayne Longpre, Barret Zoph, Yi Tay, William Fedus, Yunxuan Li, Xuezhi Wang, Mostafa Dehghani, Siddhartha Brahma, Albert Webson, Shixiang Shane Gu, Zhuyun Dai, Mirac Suzgun, Xinyun Chen, Aakanksha Chowdhery, Alex Castro-Ros, Marie Pellat, Kevin Robinson, Dasha Valter, Sharan Narang, Gaurav Mishra, Adams Yu, Vincent Zhao, Yanping Huang, Andrew Dai, Hongkun Yu, Slav Petrov, Ed H. Chi, Jeff Dean, Jacob Devlin, Adam Roberts, Denny Zhou, Quoc V. Le, and Jason Wei. Scaling instruction-finetuned language models. In *arXiv preprint arXiv: 2210.11416*, 2022.

Niv Cohen, Rinon Gal, Eli A. Meirom, Gal Chechik, and Yuval Atzmon. “this is my unicorn, fluffy”: Personalizing frozen vision-language representations. In *ECCV*, 2022.

Marco Cuturi. Sinkhorn distances: Lightspeed computation of optimal transport. In *NeurIPS*, 2013.

Abhishek Das, Satwik Kottur, Khushi Gupta, Avi Singh, Deshraj Yadav, José M. F. Moura, Devi Parikh, and Dhruv Batra. Visual dialog. In *CVPR*, 2017.

Jacob Devlin, Ming-Wei Chang, Kenton Lee, and Kristina Toutanova. Bert: Pre-training of deep bidirectional transformers for language understanding. In *NAACL*, 2019.

Jiali Duan, Liqun Chen, Son Tran, Jinyu Yang, Yi Xu, Belinda Zeng, and Trishul Chilimbi. Multi-modal alignment using representation codebook. In *CVPR*, 2022.

Constantin Eichenberg, Sidney Black, Samuel Weinbach, Letitia Parcalabescu, and Anette Frank. Magma–multimodal augmentation of generative models through adapter-based finetuning. In *EMNLP*, 2022.

Yash Goyal, Tejas Khot, Douglas Summers-Stay, Dhruv Batra, and Devi Parikh. Making the v in vqa matter: Elevating the role of image understanding in visual question answering. In *CVPR*, 2017.

Jiaxian Guo, Junnan Li, Dongxu Li, Anthony Meng Huat Tiong, Boyang Li, Dacheng Tao, and Steven C.H. Hoi. From images to textual prompts: Zero-shot vqa with frozen large language models. In *CVPR*, 2023.

Jack Hessel, Ari Holtzman, Maxwell Forbes, Ronan Le Bras, and Yejin Choi. Clipscore: A reference-free evaluation metric for image captioning. In *EMNLP*, 2021.

John Hewitt and Christopher D. Manning. A structural probe for finding syntax in word representations. In *NAACL*, 2019.

Zhicheng Huang, Zhaoyang Zeng, Bei Liu, Dongmei Fu, and Jianlong Fu. Pixel-bert: Aligning image pixels with text by deep multi-modal transformers. In *CoRR*, 2020.

Ganesh Jawahar, Benoît Sagot, and Djamé Seddah. What does bert learn about the structure of language? In *ACL*, 2019.

Chao Jia, Yinfei Yang, Ye Xia, Yi-Ting Chen, Zarana Parekh, Hieu Pham, Quoc V. Le, Yunhsuan Sung, Zhen Li, and Tom Duerig. Scaling up visual and vision-language representation learning with noisy text supervision. In *ICML*, 2021.

Jing Yu Koh, Ruslan Salakhutdinov, and Daniel Fried. Grounding language models to images for multimodal inputs and outputs. In *ICML*, 2023.

Junnan Li, Ramprasaath R, Selvaraju, Akhilesh Deepak Gotmare, Shafiq Joty, Caiming Xiong, and Steven Hoi. Align before fuse: Vision and language representation learning with momentum distillation. In *NeurIPS*, 2021.

Junnan Li, Dongxu Li, Caiming Xiong, and Steven Hoi. Blip: Bootstrapping language-image pre-training for unified vision-language understanding and generation. In *ICML*, 2022.

Junnan Li, Dongxu Li, Silvio Savarese, and Steven Hoi. Blip2: Bootstrapping language-image pre-training with frozen image encoders and large language models. In *ICML*, 2023.

Weixin Liang, Yuhui Zhang, Yongchan Kwon, Serena Yeung, and James Zou. Mind the gap: understanding the modality gap in multi-modal contrastive representation learning. In *NeurIPS*, 2022.

Chin-Yew Lin. Rouge: A package for automatic evaluation of summaries. In *Text Summarization Branches Out*, 2004.

Tsung-Yi Lin, Michael Maire, Serge Belongie, James Hays, Pietro Perona, Deva Ramanan, Piotr Dollár, and C. Lawrence Zitnick. Microsoft coco: Common objects in context. In *ECCV*, 2014.

Haotian Liu, Chunyuan Li, Qingyang Wu, and Yong Jae Lee. Visual instruction tuning. In *NeurIPS*, 2023a.

Nelson F. Liu, Matt Gardner, Yonatan Belinkov, Matthew E. Peters, and Noah A. Smith. Linguistic knowledge and transferability of contextual representations. In *NAACL*, 2019.

Yang Liu, Zhipeng Zhou, and Baigui Sun. Cot: Unsupervised domain adaptation with clustering and optimal transport. In *CVPR*, 2023b.

Jiasen Lu, Dhruv Batra, Devi Parikh, and Stefan Lee. Vilbert: Pretraining task-agnostic visiolinguistic representations for vision-and-language tasks. In *NeurIPS*, 2019.

Jack Merullo, Louis Castricato, Carsten Eickhoff, and Ellie Pavlick. Linearly mapping from image to text space. In *ICLR*, 2023.

Ron Mokady, Amir Hertz, and Amit H. Bermano. Clipcap: Clip prefix for image captioning. In *arXiv preprint arXiv: 2111.09734*, 2021.

Kishore Papineni, Salim Roukos, Todd Ward, and Wei-Jing Zhu. Bleu: A method for automatic evaluation of machine translation. In *ACL*, 2002.

Roma Patel and Ellie Pavlick. Mapping language models to grounded conceptual spaces. In *ICLR*, 2022.

Alec Radford, Karthik Narasimhan, Tim Salimans, and Ilya Sutskever. Improving language understanding by generative pre-training. Technical report, OpenAI, 2018.

Alec Radford, Jeffrey Wu, Rewon Child, David Luan, Dario Amodei, and Ilya Sutskever. Language models are unsupervised multitask learners. Technical report, OpenAI, 2019.

Alec Radford, Jong Wook Kim, Chris Hallacy, Aditya Ramesh, Gabriel Goh, Sandhini Agarwal, Girish Sastry, Amanda Askell, Pamela Mishkin, Jack Clark, Gretchen Krueger, and Ilya Sutskever. Learning transferable visual models from natural language supervision. In *ICLR*, 2021.

Colin Raffel, Noam Shazeer, Adam Roberts, Katherine Lee, Sharan Narang, Michael Matena, Yanqi Zhou, Wei Li, and Peter J. Liu. Exploring the limits of transfer learning with a unified text-to-text transformer. *JMLR*, 21(140):1–67, 2020.

Tim Sainburg, Leland McInnes, and Timothy Q Gentner. Parametric umap embeddings for representation and semi-supervised learning. *Neural Computation*, 33(11), 2021.

Piyush Sharma, Nan Ding, Sebastian Goodman, and Radu Soricut. Conceptual captions: A cleaned, hypernymed, image alt-text dataset for automatic image captioning. In *ACL*, 2018.

Yi-Lin Sung, Jaemin Cho, and Mohit Bansal. Vl-adapter: Parameter-efficient transfer learning for vision-and-language tasks. In *CVPR*, 2022.

Hao Tan and Mohit Bansal. Lxmert: Learning cross-modality encoder representations from transformers. In *EMNLP*, 2019.

Ian Tenney, Dipanjan Das, and Ellie Pavlick. Bert rediscovers the classical nlp pipeline. In *ACL*, 2019.

Yoad Tewel, Yoav Shalev, Idan Schwartz, and Lior Wolf. Zerocap: Zero-shot image-to-text generation for visual-semantic arithmetic. In *CVPR*, 2022.

Maria Tsimpoukelli, Jacob Menick, Serkan Cabi, S. M. Ali Eslami, Oriol Vinyals, and Felix Hill. Multimodal few-shot learning with frozen language models. In *NeurIPS*, 2021.

Aaron van den Oord, Yazhe Li, and Oriol Vinyals. Representation learning with contrastive predictive coding. In *arXiv preprint arXiv: 1807.03748*, 2018.

Ramakrishna Vedantam, C. Lawrence Zitnick, and Devi Parikh. Cider: Consensus-based image description evaluation. In *CVPR*, 2015.

Ivan Vulić, Edoardo M. Ponti, Robert Litschko, Goran Glavaš, and Anna Korhonen. Probing pretrained language models for lexical semantics. In *ACL*, 2019.

Ben Wang and Aran Komatsuzaki. Gpt-j-6b: A 6 billion parameter autoregressive language model. 2021. URL `https://github.com/kingoflolz/mesh-transformer-jax`.

Zhirong Wu, Yuanjun Xiong, Stella X. Yu, and Dahua Lin. Unsupervised feature learning via non-parametric instance discrimination. In *CVPR*, 2018.

Renjun Xu, Pelen Liu, Liyan Wang, Chao Chen, and Jindong Wang. Reliable weighted optimal transport for unsupervised domain adaptation. In *CVPR*, 2020.

Youngjae Yu, Jiwan Chung, Heeseung Yun, Jack Hessel, Jae Sung Park, Ximing Lu, Rowan Zellers, Prithviraj Ammanabrolu, Ronan Le Bras, Gunhee Kim, and Yejin Choi. Multimodal knowledge alignment with reinforcement learning. In *arXiv preprint arXiv:2205.12630*, 2022.

Susan Zhang, Stephen Roller, Naman Goyal, Mikel Artetxe, Moya Chen, Shuohui Chen, Christopher Dewan, Mona Diab, Xian Li, Xi Victoria Lin, Todor Mihaylov, Myle Ott, Sam Shleifer, Kurt Shuster, Daniel Simig, Punit Singh Koura, Anjali Sridhar, Tianlu Wang, and Luke Zettlemoyer. Opt: Open pre-trained transformer language models. In *arXiv preprint arXiv: 2205.01068*, 2022.

Hyperparameter	Model			
	BEiT-OPT$_{1.3B}$	BEiT-T5$_{Base}$	CLIP-OPT$_{1.3B}$	CLIP-T5$_{Base}$
Warmup steps	1.5K	3K	1.5K	3K
Learning rate	1e-4	5e-3	1e-4	5e-3
Final learning rate	0			
Batch size	128	256	128	256
Total steps	30K	15K	30K	15K
AdamW β	(0.9, 0.999)			
Text prompt	`A photo of`			

Table 4: Hyperparameters for training VLAP corresponding to each image encoders and LLMs.

A TRAINING DETAILS

We provide hyperparameters used during training in Table 4.

B INFERENCE DETAILS

As demonstrated in Section 4, VLAP presents the emerging flexibility and applicability to various vision-language tasks. While VLAP is trained on a unified training procedure, the inference provides output with a slightly different scheme with respect to the task. In Figure 5, we provide illustrations for inference corresponding to each task to prevent confusion and help clearly understand the inference procedure of VLAP.

B.1 IMAGE CAPTIONING

For image captioning, VLAP provides the text description for the given image. As shown in Figure 5a, we use "`A photo of`" as the input text prompt.

B.2 VISUAL QUESTION ANSWERING

For VQA, we use "`Question:` { } `Short answer:`" as the input text prompt.

B.3 CROSS-MODAL RETRIEVAL

Visual dialog (IT2T retrieval). In visual dialog (IT2T retrieval), the image and the sequence of question-answer dialog are given as inputs. We prepend the visual representations to text representations of the dialog sequence and feed them into LLMs. As shown in Figure 5c, we measure the cross-entropy loss between the generated output and the answer candidates, and select the one with the lowest loss as the prediction.

Text-to-image (T2I) retrieval. Different from the other tasks, VLAP does not utilize the generative ability of LLMs for T2I retrieval. As shown in Figure 5d, we first extract the visual representations for all images in the dataset. We extract the text representations for the input dialog and directly measure the similarity between the text representations and all visual representations. We select the target image with the highest similarity.

C ADDITIONAL RESULTS

C.1 IMAGE CAPTIONING

We provide the zero-shot image captioning performance on the NoCaps (Agrawal et al., 2019) and MSCOCO (Lin et al., 2014) datasets with additional evaluation metrics, including BLEU (Papineni et al., 2002), METEOR (Banerjee & Lavie, 2005), ROUGE (Lin, 2004), and SPICE (Anderson et al., 2016). As shown in Table 5, VLAP with CLIP ViT-B/32 (Radford et al., 2021) and two

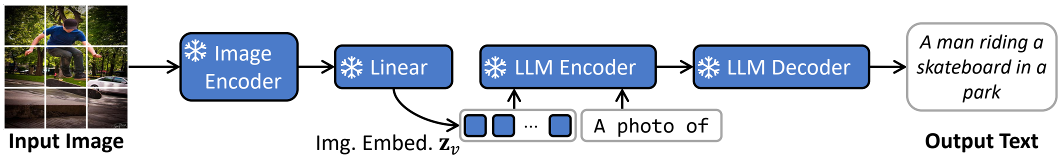

(a) Image captioning

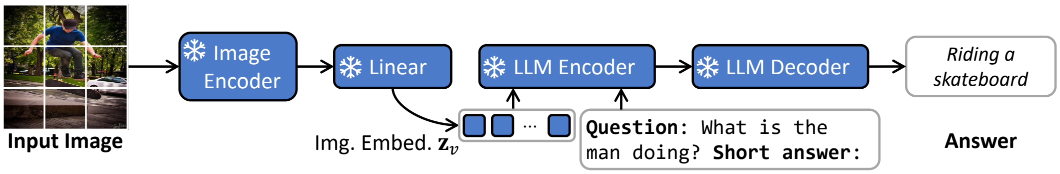

(b) Visual question answering

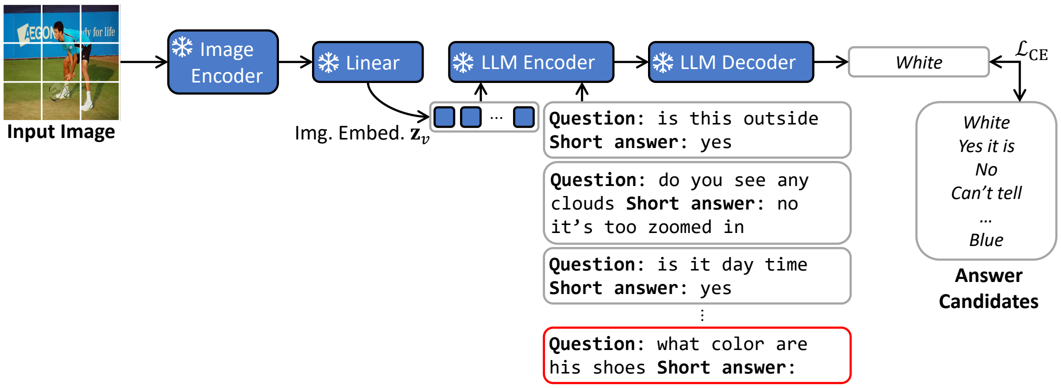
Input Image
Image Encoder
Linear
LLM Encoder
LLM Decoder
White
$\mathcal{L}_{\text{CE}}$
Img. Embed. $\mathbf{z}_v$
Question: is this outside Short answer: yes
Question: do you see any clouds Short answer: no it's too zoomed in
Question: is it day time Short answer: yes
Question: what color are his shoes Short answer:
White
Yes it is
No
Can't tell
…
Blue
Answer Candidates

(c) Visual dialog (image-and-text to text (IT2T) retrieval)

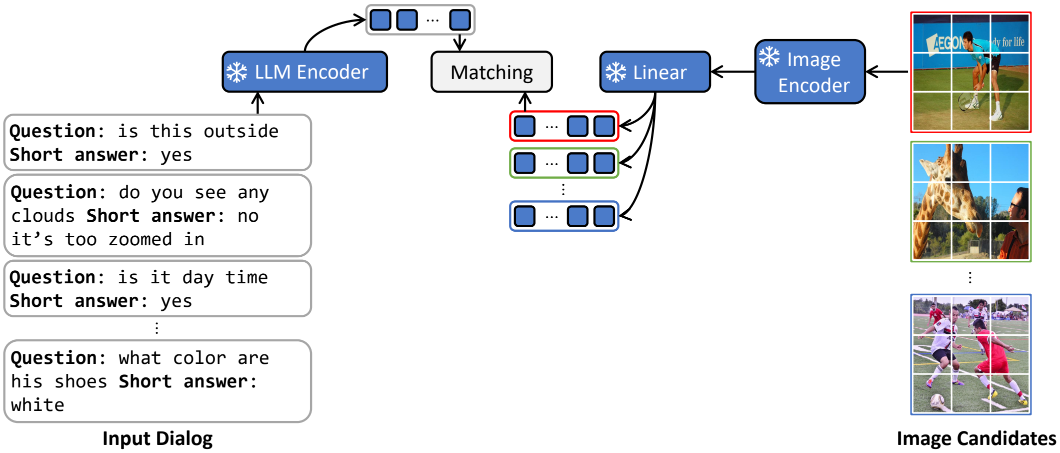
LLM Encoder
Matching
Linear
Image Encoder
Question: is this outside Short answer: yes
Question: do you see any clouds Short answer: no it's too zoomed in
Question: is it day time Short answer: yes
Question: what color are his shoes Short answer: white
Input Dialog
Image Candidates

(d) Text-to-image retrieval

Figure 5: Illustrations for the inference on (a) image captioning, (b) visual question answering, (c) visual dialog, and (d) text-to-image retrieval.

LLMs (Zhang et al., 2022; Raffel et al., 2020) persistently outperform the previous methods, including MAGMA (Eichenberg et al., 2022), LiMBeR (Merullo et al., 2023), and FROMAGe (Koh et al., 2023). In addition, VLAP with BEiT (Bao et al., 2022) achieves comparable or better performance on several evaluation metrics than the previous approaches with CLIP image encoders, demonstrating the effectiveness of the proposed assignment prediction objective.

Method	Vis. Encoder	Lang. Model	BLEU-1	BLEU-2	BLEU-3	BLEU-4	METEOR	ROUGE	SPICE
MAGMA	CLIP RN50x16	GPT-J	0.432	0.300	0.203	0.137	0.159	0.376	0.117
LiMBeR	BEiT	GPT-J	0.319	0.187	0.105	0.060	0.106	0.299	0.093
LiMBeR	CLIP RN50x16	GPT-J	0.400	0.278	0.187	0.126	0.161	0.376	0.121
FROMAGe	CLIP ViT-L/14	$\text{OPT}_{6.7\text{B}}$	0.477	0.293	0.172	0.102	0.287	-	-
VLAP	BEiT	$\text{OPT}_{1.3\text{B}}$	0.449	0.348	0.225	0.174	0.280	0.369	0.118
VLAP	BEiT	T5_{Base}	0.458	0.357	0.266	0.176	0.287	0.382	0.120
VLAP	CLIP ViT-B/32	$\text{OPT}_{1.3\text{B}}$	0.567	0.429	0.343	0.291	0.310	0.482	0.135
VLAP	CLIP ViT-B/32	T5_{Base}	**0.571**	**0.437**	**0.348**	**0.297**	**0.311**	**0.487**	**0.137**

Table 5: Performance comparisons between MAGMA (Eichenberg et al., 2022), LiMBeR (Merullo et al., 2023), FROMAGe (Koh et al., 2023), and VLAP for zero-shot image captioning on the NoCaps and MSCOCO datasets. We report the architectures of visual and language models, CIDEr-D (Vedantam et al., 2015), CLIP-Score, and RefCLIP Score (Hessel et al., 2021).

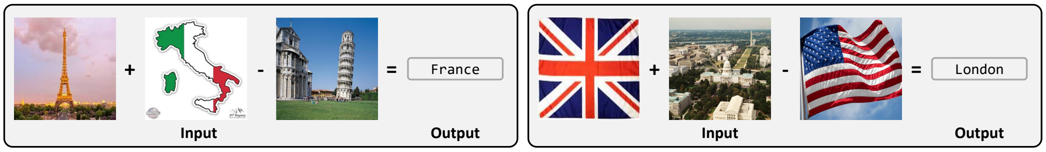

(a) Building→Country (b) Country→Capital

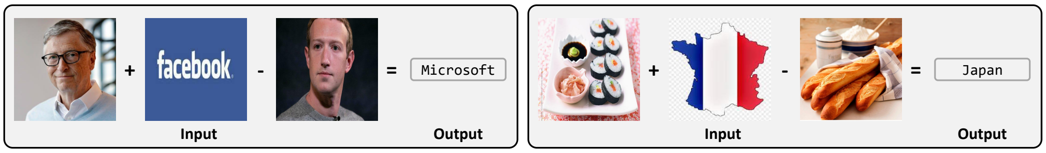

(c) CEO→Company (d) Food→Country

Figure 6: Illustrations for the visual relation benchmark.

C.2 VISUAL SEMANTIC ARITHMETIC

Performance on the visual relation benchmark. To further explore the capability in visual semantic arithmetic of VLAP, we evaluate VLAP on the visual relation (VR) benchmark (Tewel et al., 2022). The VR benchmark consists of a total of 320 relations, including building→country, country→capital, CEO→company, food→country, and leader→country. Since the relation of leader→country includes out-of-date information (e.g. 'Obama'-'USA'), we exclude it from this experiment. We illustrate examples for the VR benchmark in Figure 6. In Table 6, we compare the performance between VLAP, ClipCap (Mokady et al., 2021), and ZeroCap (Tewel et al., 2022) in terms of BLEU-1 (Papineni et al., 2002), Recall@5, and CLIP-Score (Hessel et al., 2021), following Tewel et al. (2022). For fair comparisons, we identically use CLIP ViT-B/32 (Radford et al., 2021) as the image encoder and GPT-2 (Radford et al., 2019) as the LLM. The results show that VLAP outperforms the previous methods by large margins. In particular, we attain correlations of over 75% in all relations on the semantic distance-based metric, i.e., CLIP-Score.

Visualization. We provide UMAP visualization (Sainburg et al., 2021) for the representations to analyze the visual arithmetic of VLAP in feature space, as shown in Figure 7. The blue and green circles are the real pairs and the red circles denote the embeddings obtained by the visual arithmetic operation. For example, the images of 'the Eiffel Tower'-'France' and 'the Leaning Tower of Pisa'-'Italy' in Figure 7a have a 'building-country' relation. The direction from 'building' to 'country' can be obtained through a subtraction operation between visual features of 'Italy' and 'the Leaning Tower of Pisa.' The summation of this direction with the embedding of 'the Eiffel Tower' allows us to derive the embedding corresponding to the same relation as 'building-country,' i.e., 'France.' In practice, the embedding obtained by visual arithmetic operations is close to the image of 'France' in the feature space and the LLM generates the caption of '`A photo of France`' with the embedding obtained by visual arithmetic operations. Similarly, the direction for the relation of

Method	Building → Country			Country → Capital			CEO → Company			Food → Country		
	B@1	R@5	CLIP-S	B@1	R@5	CLIP-S	B@1	R@5	CLIP-S	B@1	R@5	CLIP-S
ClipCap	0.003	0.035	0.24	0.0	0.0	0.22	0.004	0.005	0.18	0.0	0.0	0.24
ZeroCap	0.1	0.32	0.7	0.14	0.32	0.68	0.1	0.3	0.64	0.03	0.33	0.66
VLAP	**0.3**	**0.53**	**0.87**	**0.46**	**0.62**	**0.89**	**0.25**	**0.5**	**0.75**	**0.17**	**0.5**	**0.81**

Table 6: Performance comparisons between ClipCap (Mokady et al., 2021), ZeroCap (Tewel et al., 2022), and VLAP for visual semantic arithmetic on the Visual Relation dataset. Following Tewel et al. (2022), we report BLEU-1, R@5, and CLIP-Score.

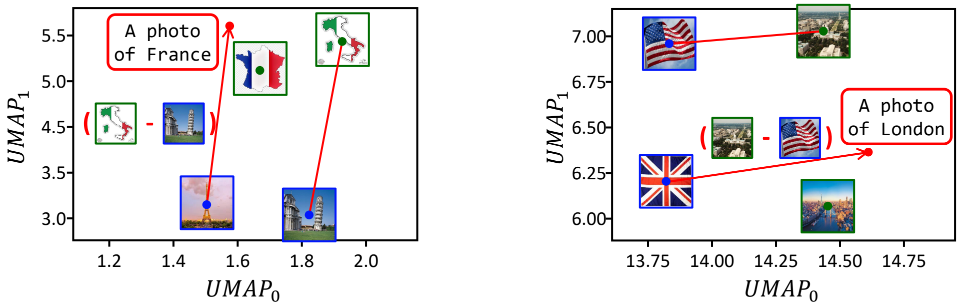

(a) Building→Country

(b) Country→Capital

Figure 7: UMAP visualization (Sainburg et al., 2021) of selected examples from the visual relation benchmark.

'country-capital' can be obtained by subtracting the image of 'USA' from the image of 'Washington.' The LLM generates the caption '`A photo of London`' from the embedding of the summation of the direction and the image of 'England.'

D ABALATION STUDY

D.1 LOSS FUNCTION

λ_{map}	λ_{cap}	MSCOCO		
		CIDEr-D	CLIP-S	Ref-S
0	1	51.7	72.1	76.3
0.2	0.8	62.3	80.3	85.0
0.4	0.6	68.1	84.8	89.2
0.5	0.5	69.6	86.3	91.6
0.6	0.4	69.9	86.7	91.8
0.8	0.2	64.5	83.1	87.8
1	0	49.6	72.4	76.1

(a) Different ratios between λ_{map} and λ_{map}

Training Objective				MSCOCO		
$\mathcal{L}_{cap}$	$\mathcal{L}_{ITM}$	$\mathcal{L}_{ITC}$	$\mathcal{L}_{map}$	CIDEr-D	CLIP-S	Ref-S
✓				51.7	72.1	76.3
✓	✓			58.4	78.2	81.7
✓	✓	✓		61.8	79.0	82.3
✓	✓	✓	✓	65.7	82.5	85.8
✓			✓	69.9	86.7	91.8

(b) Combinations of objectives

Table 7: Zero-shot image captioning performance on MSCOCO (Lin et al., 2014) corresponding to (a) different ratios between the balancing parameters (i.e., $\lambda_{map} : \lambda_{cap}$) and (b) combinations of learning objectives.

To validate the effectiveness of each component in VLAP, we evaluate the zero-shot image captioning performance of VLAP trained with various combinations of learning objectives on MSCOCO (Lin et al., 2014). All experiments are conducted with CLIP ViT-B/32 (Radford et al., 2021) and $\text{OPT}_{1.3\text{B}}$ (Zhang et al., 2022) as the vision model and LLM, respectively.

Effectiveness of λ_{map} and λ_{cap}. The balancing parameters in equation 7 control the importance of $\mathcal{L}_{map}$ and $\mathcal{L}_{cap}$. In Table 7a, we report the performance corresponding to different ratios between λ_{map} and λ_{cap} while keeping the sum of two terms as 1. In the first row (i.e., $\lambda_{map} : \lambda_{cap} = 0 : 1$),

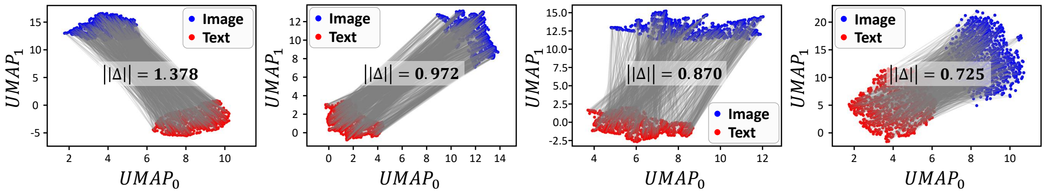

(a) Before training (b) w/$\mathcal{L}_{\text{cap}}$ (c) w/$\mathcal{L}_{\text{cap}} + \mathcal{L}_{\text{ITM}} + \mathcal{L}_{\text{ITC}}$ (d) w/$\mathcal{L}_{\text{cap}}$+$\mathcal{L}_{\text{map}}$

Figure 8: UMAP visualization (Sainburg et al., 2021) of visual and text representations corresponding to the combinations of objectives.

the final objective is $\mathcal{L} = \mathcal{L}_{\text{cap}}$, which is equivalent to the language modeling objective of LiMBeR (Merullo et al., 2023) and the first stage of LLaVA (Liu et al., 2023a). With this objective only, VLAP performs significantly poorly, attaining 51.7 of CIDEr-D. While VLAP with only assignment prediction (i.e., $\mathcal{L} = \mathcal{L}_{\text{map}}$) performs worse than with only language modeling, $\mathcal{L}_{\text{map}}$ improves the performance even by a small portion, showing a performance improvement of 10.6 on the CIDEr-D score. Increasing the ratio of λ_{map} gradually improves the performance, achieving the best performance of 69.9 with $\lambda_{\text{map}} : \lambda_{\text{cap}} = 0.6 : 0.4$. Thus, the results demonstrate the effectiveness of the proposed assignment prediction objective while emphasizing the necessity of the language modeling objective to leverage the generative ability of LLMs.

With additional objectives. Image-text contrastive (ITC) and image-text matching (ITM) objectives, which directly compare image and text representations, have been proposed for cross-modal alignment (Li et al., 2021; 2022; 2023). We modify the ITC and ITM objectives to evaluate the performance of VLAP trained with these objectives. For ITC, we contrast the similarity between averaged image and text representations (i.e., $\bar{\mathbf{Z}}^v$ and $\bar{\mathbf{Z}}^t$) of a positive pair against those of negative pairs in a batch. The ITC objective $\mathcal{L}_{\text{ITC}}$ is defined as the cross-entropy loss between pairwise similarities and the groundtruth one-hot similarities, where the positive pair has 1 and the negative pairs have 0. For ITM, we learn an additional linear layer as a binary classifier to determine whether an image-text pair is matched or not. We concatenate the averaged image and text representations and feed them into the classifier with the softmax activation. Following Li et al. (2021; 2022; 2023), we also employ the hard negative sampling strategy based on the pairwise similarity. The ITM objective $\mathcal{L}_{\text{ITM}}$ is defined as the binary cross-entropy loss.

We evaluate VLAP trained with different combinations of learning objectives: (1) $\mathcal{L}_{\text{cap}}$; (2) $\mathcal{L}_{\text{cap}} + \mathcal{L}_{\text{ITM}}$; (3) $\mathcal{L}_{\text{cap}} + \mathcal{L}_{\text{ITM}} + \mathcal{L}_{\text{ITC}}$; (4) $\mathcal{L}_{\text{cap}} + \mathcal{L}_{\text{ITM}} + \mathcal{L}_{\text{ITC}} + \mathcal{L}_{\text{map}}$; and (5) the original objective of VLAP, $\mathcal{L}_{\text{cap}} + \mathcal{L}_{\text{map}}$. As shown in Table 7b, $\mathcal{L}_{\text{ITM}}$ and $\mathcal{L}_{\text{ITC}}$ contribute to performance improvement with $\mathcal{L}_{\text{cap}}$, achieving 58.4 in (2) and 61.8 in (3). However, we notice that the ITM and ITC objectives hurt overall performance, as shown in the performance comparison between (4) and (5). We argue that ITM and ITC solely focus on direct pairwise comparisons without considering the semantic correlation between predefined two embedding spaces. Namely, they enforce instance discrimination and encourage the existence of the modality gap (Liang et al., 2022).

To further analyze the impact of each objective, we also provide UMAP visualization (Sainburg et al., 2021) with the modality gap distance, as shown in Figure 8. Note that the blue and red circles represent image and text embeddings and the gray lines refer to image-text pairs, respectively. Formally, the modality gap Δ is defined as the difference between the center of visual and text representations (Liang et al., 2022):

$$\Delta = \frac{1}{n}\sum_{i=1}^{n} \bar{\mathbf{z}}_i^v - \frac{1}{n}\sum_{i=1}^{n} \bar{\mathbf{z}}_i^t, \tag{8}$$

where n is the total number of image-text pairs, $\bar{\mathbf{z}}_i^v$, and $\bar{\mathbf{z}}_i^t$ are the i-th averaged visual and text representations. As shown in Figure 8a, we can observe the obvious modality gap before training, which separates two modality embeddings, and the default gap distance between CLIP ViT-B/32 and T5$_{\text{Base}}$ is $||\Delta|| = 1.378$. Although the image captioning objective $\mathcal{L}_{\text{cap}}$ (Figure 8b) and the additional objectives (Figure 8c) reduce the modality gap distance to $||\Delta|| = 0.972$ and $||\Delta|| = 0.870$, respectively, the modality gap still exists. In Figure 8d, the modality gap between two modality

	Method	$\epsilon-$MSCOCO (CIDEr-D)			
		0.1	0.05	0.01	0.005
(i)	VLAP w/o word embed.	20.4	43.8	38.9	-
(ii)	VLAP w/o word dist.	50.7	57.9	57.1	46.2
(iii)	VLAP	61.8	68.0	69.9	67.7

Table 8: Ablation study for the components in assignment prediction. We evaluate the zero-shot image captioning performance on MSCOCO (Lin et al., 2014) and report the CIDEr-D score.

Method	Vis. Encoder	Lang. Model	NoCaps (CIDEr-D)				NoCaps (All)		MSCOCO		
			In	Out	Near	All	CLIP-S	Ref-S	CIDEr-D	CLIP-S	Ref-S
MAGMA	CLIP RN50x16	GPT-J	30.4	43.4	36.7	38.7	74.3	78.7	47.5	75.3	79.6
LiMBeR	CLIP RN50x16	GPT-J	34.3	48.4	41.6	43.9	74.7	79.4	54.9	76.2	80.4
VLAP	CLIP ViT-B/32	$\text{OPT}_{1.3\text{B}}$	48.2	62.7	59.3	61.3	84.8	88.5	69.9	86.7	91.8
VLAP	CLIP ViT-B/32	T5_{Base}	48.3	62.7	59.6	61.6	85.1	88.7	69.4	87.6	92.0
VLAP	CLIP RN50x16	GPT-J	**53.8**	**67.5**	**65.7**	**64.5**	**88.3**	**90.1**	**75.3**	**90.6**	**92.2**

Table 9: Performance comparisons between MAGMA (Eichenberg et al., 2022), LiMBeR (Merullo et al., 2023), and VLAP for zero-shot image captioning. We report the architectures of visual and language models, CIDEr-D, CLIP-Score, and RefCLIP-Score.

embeddings is significantly relaxed and the gap distance is further reduced to $||\Delta|| = 0.725$ with our assignment prediction objective.

D.2 OPTIMAL TRANSPORT

The assignment prediction of VLAP mainly differs from the previous optimal transport-based (or clustering-based) approaches (Asano et al., 2020b; Caron et al., 2020; Asano et al., 2020a; Duan et al., 2022) in the following aspects: (1) defining a fixed central space instead of a learnable central space (i.e., prototypes) and (2) defining the transportation polytope with the word distribution of the training dataset instead of the equipartition assumption. We conduct additional experiments to validate the effectiveness of each component in our assignment prediction. As shown in Table 8, we evaluate each model for zero-shot image captioning (CIDEr-D) on MSCOCO corresponding to various ϵ. In (i) "VLAP w/o word embed.", we first train VLAP with learnable prototypes as in Asano et al. (2020b); Caron et al. (2020); Asano et al. (2020a); Duan et al. (2022). In this setting, we define 3K prototypes following Caron et al. (2020) and apply the equipartition assumption. In (ii) "VLAP w/o word dist.", we also verify the effectiveness of the word distribution. In this setting, we use the word embeddings as a fixed central space and perform the optimal transport with the equipartition assumption. The comparison between (i) and (ii) shows that the word embedding achieves substantial performance improvement, demonstrating the effectiveness of the word embedding. In addition, VLAP without the word distribution is highly sensitive to the entropy parameter ϵ, showing large performance fluctuation depending on the value of ϵ. The comparison between (ii) and (iii) original VLAP shows that the transportation polytope with the word distribution achieves additional performance improvement and provides more robust performance regarding ϵ.

D.3 DIFFERENT BACKBONES

While we used the transformer-based vision models (i.e., CLIP ViT-B/32 and BEiT) and the relatively small scale of LLMs (i.e., $\text{OPT}_{1.3\text{B}}$ and T5_{Base}) in the main paper, VLAP can be easily applied to other publicly available vision models and LLMs. Following MAGMA (Eichenberg et al., 2022) and LiMBeR (Merullo et al., 2023), we additionally evaluate VLAP with the CNNs-based vision model (i.e., CLIP RN50x16 (Radford et al., 2021)) and the larger LLM (i.e., GPT-J (Wang & Komatsuzaki, 2021), which has 6B parameters) for zero-shot image captioning on NoCaps and MSCOCO. Not surprisingly, as shown in Table 9, VLAP with the larger LLM performs better than the smaller LLMs, significantly outperforming MAGMA and LiMBeR by large margins across all metrics with the same backbones.

Finetune Data	Vis. Encoder	Lang. Model	NoCaps (CIDEr-D)	MSCOCO (CIDEr-D)	VQA2 ($n = 0$)	IT2T (R@1)	T2I (R@1)
CC3M	CLIP ViT-B/32	T5$_{\text{Base}}$	61.6	69.4	41.1	21.1	26.9
CC12M	CLIP ViT-B/32	T5$_{\text{Base}}$	62.4	70.1	41.3	23.0	28.2

Table 10: Performance comparisons of VLAP according to the pretraining dataset for several zero-shot vision-language tasks.

D.4 PRETRAINING DATASET

VLAP formulates the transportation polytope in word assignment with the marginal distribution of words in a training dataset. Therefore, we hypothesize that pretraining VLAP on a larger-scale dataset, which covers a wider range of word distribution, has the potential to lead to better performance. To demonstrate this, we train VLAP on the CC12M Changpinyo et al. (2021) dataset that contains about 4 times more images than CC3M and evaluate the performance on several zero-shot vision-language tasks, including image captioning, visual question answering (VQA), and cross-modal retrieval. In Table 10, we present performance comparisons of VLAP according to the pretraining dataset for each task. The results show that increasing the amount of training data consistently improves the zero-shot capability of VLAP across tasks, supporting observations from previous works Li et al. (2021; 2022).